ELSEVIER

Journal of Alloys and Compounds 317–318 (2001) 92–97

Journal of ALLOYS AND COMPOUNDS

www.elsevier.com/locate/jallcom

Neutron diffraction studies of Zr-containing intermetallic hydrides. Cubic $Zr_3V_3B_{0.24}O_{0.36}D_{8.0}$ and $Zr_3V_3B_{0.40}O_{0.60}D_{6.4}$ with filled η_1-type structures

V.A. Yartys[a,b,*], A.B. Riabov[b], B.C. Hauback[a]

[a]*Institute for Energy Technology, P.O. Box 40, Kjeller, N-2027 Norway*

[b]*Metal Hydrides Department, Karpenko Physico-Mechanical Institute of the National Academy of Sciences of Ukraine, 5, Naukova Str., Lviv 290601, Ukraine*

Abstract

The deuterides $Zr_3V_3B_{0.24}O_{0.36}D_{8.0}$ and $Zr_3V_3B_{0.40}O_{0.60}D_{6.4}$ with cubic structures [space group $Fd\bar{3}m$ (No. 227)] related to η_1-(Fe_3W_3C) type have been studied by powder X-ray and neutron diffraction. The transition from the alloys to the corresponding deuterides gives a redistribution of the O/B atoms between two available types of zirconium octahedra, from 16*d* (1/2, 1/2, 1/2) into the 8*b* (7/8, 3/8, 7/8) sites. A correlation between occupancy/vacancy of the Zr_6 octahedra and the structure of the deuterium sublattice has been established. This explains the significant differences between the deuterides studied in this work and the previously reported, chemically similar $Zr_3V_3OD_{4.93}$.

Keywords: Powder neutron diffraction; Zirconium; Vanadium; Boron oxide; Deuteride

1. Introduction

Boron oxide doping favours the hydrogenation properties of Zr–V alloys [1,2]. Both increased hydrogen sorption rates, even at low operating pressures, and high H-storage capacities, exceeding 2.5 wt% H, are beneficial characteristics of such alloys [2].

A recent metallographic characterisation and powder neutron diffraction (PND) study, focusing on the effect of B_2O_3 addition on the hydrogenation behaviour of the Zr–V system, showed that Zr–V–B_2O_3 alloys with compositions $Zr_3V_3B_{0.24}O_{0.36}$ and $Zr_3V_3B_{0.40}O_{0.60}$ contain η_1-(Fe_3W_3C) type face centred cubic oxyboride $Zr_3V_3(B,O)$ as the main phase constituent ($a=12.\underline{1}607(2)$ and 12.1705(4) Å, respectively; space group $Fd\bar{3}m$ (No. 227); $Z=16$) [3]. Two types of octahedra in the metal sublattice [regular (8*b*) and slightly distorted (16*d*)] are similar with respect to their chemical surrounding (Zr_6) and sizes ($r\sim0.7$ Å). However, for both materials only the 16*d* (1/2, 1/2, 1/2) sites were found to be nearly fully occupied by B/O atoms, while the 8*b* (7/8, 3/8, 7/8) octahedra were completely empty ($Zr_3V_3B_{0.24}O_{0.36}$) or only slightly filled ($Zr_3V_3B_{0.40}O_{0.60}$; $n=0.04$) [3].

The present PND study aims at the crystal structure of two deuterides formed from the alloys studied in Ref. [3], namely $Zr_3V_3B_{0.24}O_{0.36}D_{8.0}$ and $Zr_3V_3B_{0.40}O_{0.60}D_{6.4}$.

2. Experimental

The alloys with stoichiometric compositions $Zr_3V_3B_{0.24}O_{0.36}$ and $Zr_3V_3B_{0.40}O_{0.60}$ were prepared by argon arc melting of mixtures of high purity zirconium (99.97%), vanadium (99.5%) and boron oxide (99.9%). 99.98% ^{11}B-enriched B_2O_3 was used in order to reduce the high absorption of neutrons by natural boron. The alloys were annealed at 1273 K for 14 days and thereafter quenched into water.

Deuterium absorption by the alloys was performed at deuterium pressures 0.5–2 bar and temperatures around 673 K. Prior to passing deuterium gas (99.8% purity) into the autoclave, the samples were activated by heating under dynamic vacuum ($P<10^{-5}$ mbar) at 773 K for 1 h. Saturation was achieved in 1 h. The samples were then

*Corresponding author. Tel.: +47-63-806-453; fax: +47-63-810-920.
E-mail address: volodymyr.yartys@ife.no (V.A. Yartys).

0925-8388/01/$ – see front matter
PII: S0925-8388(00)01402-X

slowly cooled in D_2 to room temperature. The cooling was accompanied by further, but less pronounced absorption. The D-content in the deuterides was monitored by volumetric measurements and corresponds to $Zr_3V_3B_{0.24}O_{0.36}D_{8.0\pm0.1}$ and $Zr_3V_3B_{0.40}O_{0.60}D_{6.4\pm0.1}$.

Structural characterisation of the alloys and deuterides was done by powder X-ray diffraction (XRD) [Philips PW1012 diffractometer, Cu Kα radiation] and PND. PND data were collected at $T=293$ K with the PUS instrument ($\lambda=1.5492$ Å; focusing Ge(511) monochromator; $2\Theta=10$–$130°$; $\Delta2\Theta=0.05°$; 2400 data points) at the JEEP II reactor (Kjeller). The samples were placed into sealed, cylindrical vanadium holders with inner diameter 5 mm. Nuclear scattering lengths were taken from Ref. [4] ($b_{Zr}=7.16$, $b_V=-0.38$, $b_O=5.80$, $b_D=6.67$ fm) and from Ref. [5] ($b_B^{11}=6.65$ fm). The general structure analysis system (GSAS) software [4] was used in the Rietveld-type refinements. The peak shape was described by a mixed Gaussian–Lorenzian function, and the background was modelled as a cosine Fourier series polynomial.

In addition to the main phase, η_1-oxyboride, several impurity phases are present in both materials. Analysis of the PND data for the nondeuterated alloys [3] identified impurities as: α-Zr (Zr_3O), V ($VO_{0.03}$), ZrV_2 and V_3B_2. The data for the deuterated alloys are consistent with these previous observations [3]. On deuteration three of the impurity phases form deuterides: ϵ-ZrD_2 (ThD_2-type structure [6]; space group $I4/mmm$; $a=3.495$–3.521; $c=4.443$–4.482 Å), VD_2 (CaF_2 structure [7]; space group $Fm\bar{3}m$; $a=4.268$–4.270 Å) and ZrV_2D_4 (space group $I4_1/a$; $a=5.606$; $c=7.889$ Å; see Ref. [8] for further details on this structure). Since refined crystallographic characteristics of V_3B_2 (U_3Si_2 structure [9,10]; $a=5.746$–5.767; $c=3.032$–3.040 Å) agree well with the previously reported data for the deuterium-free $Zr_3V_3B_{0.24-0.40}O_{0.36-0.60}$ alloys [3], V_3B_2 does not interact with deuterium at the experimental conditions applied in the present work. In addition, trace amounts of δ-ZrO_x (NaCl structure [11]; space group $Fm\bar{3}m$; $a=4.75$ Å) were found in the $Zr_3V_3B_{0.24}O_{0.36}D_{8.0}$ sample.

3. Results and discussion

The two types of Zr_6-octahedra, 8*b* and 16*d*, form a spatial network in the η_1-type structure (Fig. 1), each sharing four (8*b*) or two (16*d*) triangular Zr_3 faces with neighbouring octahedra of the other type. Deuteration increases the radii of these octahedra by ~0.1 Å (to $r=0.79$–0.82 Å), and the distances between the centres of the 8*b* and 16*d* octahedra (2.733–2.755 Å) allow their simultaneous occupation by O/B atoms (for comparison, typical O–O, O–B and B–B distances in inorganic structures are, respectively, 2.8 Å [12], 1.3–1.7 Å [13] and 1.6–1.7 Å [14]).

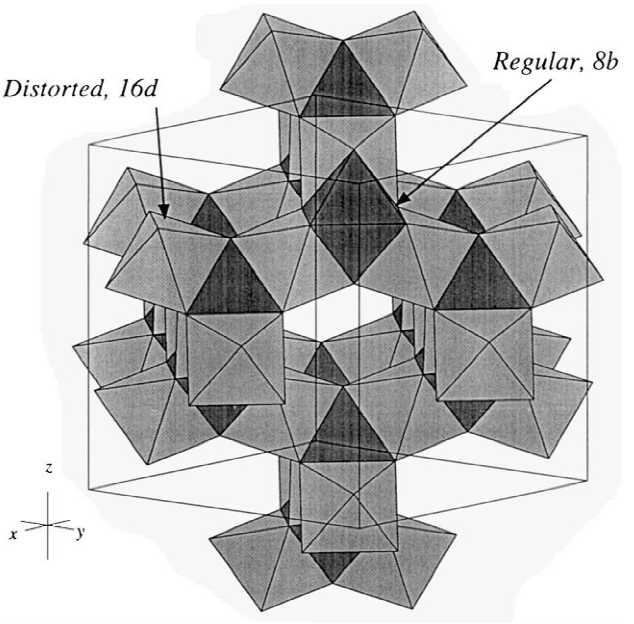

Fig. 1. The framework of two types of Zr_6 octahedra in the structure of the η_1-type phase of $Zr_3V_3B_{0.24}O_{0.36}$.

Crystal chemical analysis shows how the different octahedral (8*b* and 16*d*, both Zr_6) and tetrahedral [*D*1 (Zr_3V2), *D*2 (Zr_2V1V2), *D*3 (Zr_3V2) and *D*4 ($ZrV1V2_2$)] interstitial sites are interconnected in the structure (Fig. 2). The tetrahedral sites in the scheme correspond to the reported positions for D atoms in the known structures of η-type (Ti_2Ni-type) based deuterides, including $Zr_3V_3OD_{4.93}$ [15], $Ti_4Fe_2OD_{2.22}$ [16] and $Hf_4Fe_2D_{8.76}$ [17]. From size and chemical surrounding considerations sites *D*1 and *D*3 are advantageous for hydrogen insertion. Fig. 2 shows that both *D*1 and *D*3 sites can be completely occupied by deuterium since each interstice is not sharing common triangular faces of the same type. In contrast, only a partial occupation of the *D*2 and *D*4 interstices can take place since they are side-connected to similar interstitial positions.

Observed, calculated and difference PND pattern from the Rietveld type refinements for $Zr_3V_3B_{0.24}O_{0.36}D_{8.0}$ and

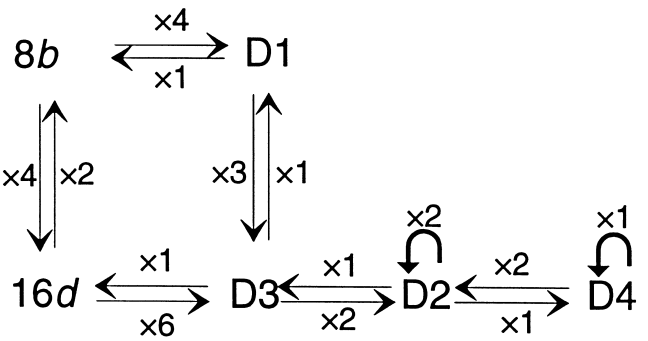

Fig. 2. Interconnection of interstitial sites in the η_1-type structure. Numbers beside the arrows show the number of triangular sides connecting neighbouring tetrahedra/octahedra.

$Zr_3V_3B_{0.40}O_{0.60}D_{6.4}$ are shown in Figs. 3 and 4. Table 1 presents the crystal structure data and interatomic distances. The metal–deuterium distances (see Table 1), Zr–D = 1.93–2.19 Å and V–D = 1.61–1.98 Å, fall into the typical range for metal hydrides. The Zr–O (2.384–2.409 Å) and Zr–B (2.392–2.454 Å) distances do not differ significantly from the nonhydrogenated η_1-oxyborides, 2.285–2.291 and 2.310 Å, respectively [3].

All four types of tetrahedral interstitial positions *D*1–*D*4 are partially filled by D atoms in both deuterides. A key common feature of all the structure models is the preferential occupation of the *D*3 Zr_3V2 tetrahedra with 35, 53, 56 and 59% of deuterium from the overall $D/Zr_3V_3(B,O)$ stoichiometry (see Table 1 for details). This is completely different from the previously reported structure of $Zr_3V_3OD_{4.93}$ (16 O in 16*d*; 8*b* non occupied; 40.4% D in *D*1; 53.4% D in *D*2; 3.2% D in *D*3 and 3.0% D in *D*4) [15] with a very small amount of deuterium in the *D*3 sites and significant population of the *D*1 and *D*2 sites.

The PND refinements show substantial changes of the 'host' sublattice upon D absorption for all η-type matrices. B and O are redistributed between the 8*b* and 16*d* sites and the 8*b* site turns out to be significantly filled in the deuterides. In addition, hydrogen insertion induces phase separation of the originally single-phase η_1-oxide into two deuterides (I and II), with different η_1-type structures. These structures are different with respect to the unit cell dimensions, the population of the 8*b* and 16*d* sites by B and O, and the D storage capacities (see Table 1). Complete occupancy by the nonmetallic atoms of the 8*b* octahedra and a corresponding small (or zero) filling of the 16*d* sites is characteristic for deuteride I. Both 8*b* and 16*d* sites are partially occupied in deuteride II. A scheme illustrating these transformations is presented in Fig. 5.

The most important features of the reported structures are the interrelationships between O/B occupancy/vacancy in the Zr_6 octahedra and D in their neighbouring tetrahedra. Based on data from Table 1 and reference data for $Zr_3V_3OD_{4.93}$ [15], two distinct models describing the structures of the hydrides of η-oxides can be suggested. These models are based on alternative occupation of O/B in the octahedral 8*b* or 16*d* sites and on the occupation of D in the tetrahedral Zr_3V2 sites (*D*3 or *D*1), which are most distant from the corresponding occupied octahedra.

Model A $8b(n = 1) + 16d(-) + D1(-) + D3(n = 1)$.

Stoichiometry $Zr_3V_3(O,B)_{0.5}D_6$.

Representative: deuteride I in $Zr_3V_3B_{0.24}O_{0.36}D_{7.96}$.

Significant occupation by D (in addition to *D*3): *D*4.

Model B $8b(-) + 16d(n = 1) + D1(n = 1) + D3(-)$.

Stoichiometry $Zr_3V_3(O,B)_{1.0}D_2$.

Representative: $Zr_3V_3OD_{4.93}$ [15].

Significant occupation by D (in addition to *D*1): *D*2.

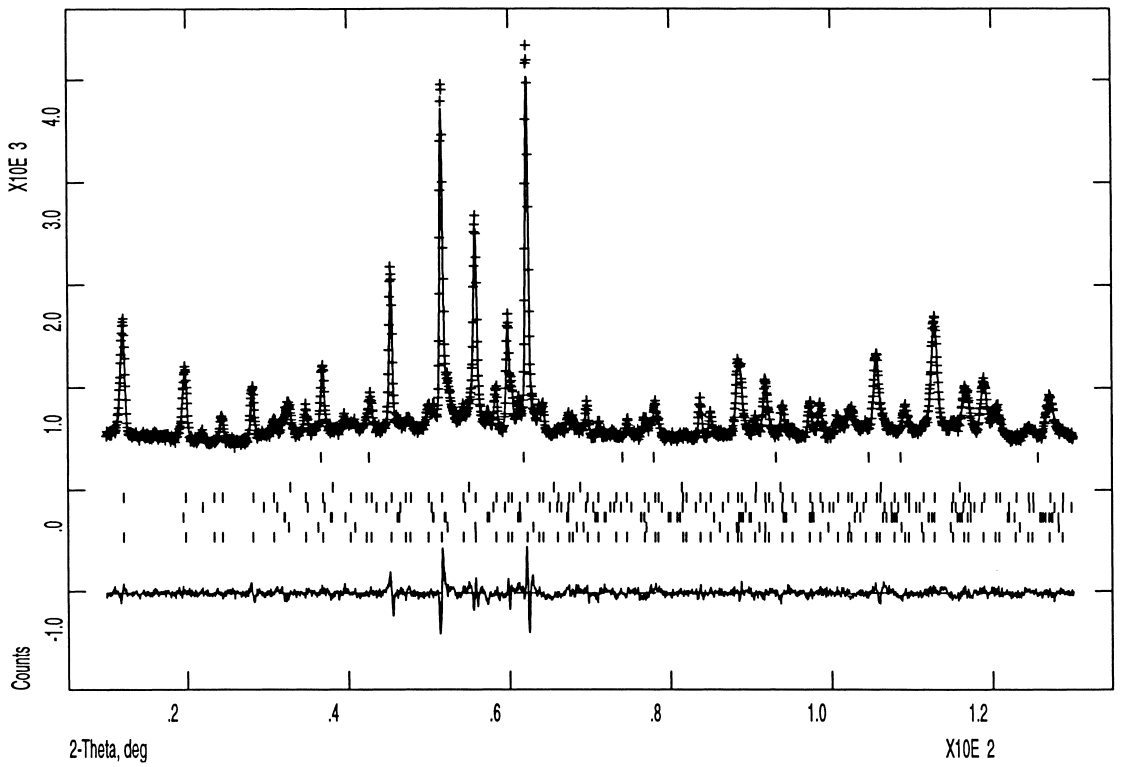

Fig. 3. Observed (+), calculated (upper line) and difference (lower line) powder neutron diffraction profile for $Zr_3V_3B_{0.24}O_{0.36}D_{7.96}$. The positions of peaks of the constituent phases are marked (from bottom to top): deuteride I, ϵ-ZrD_2, ZrV_2D_4, V_3B_2, deuteride II, δ-ZrO_x and VD_2.

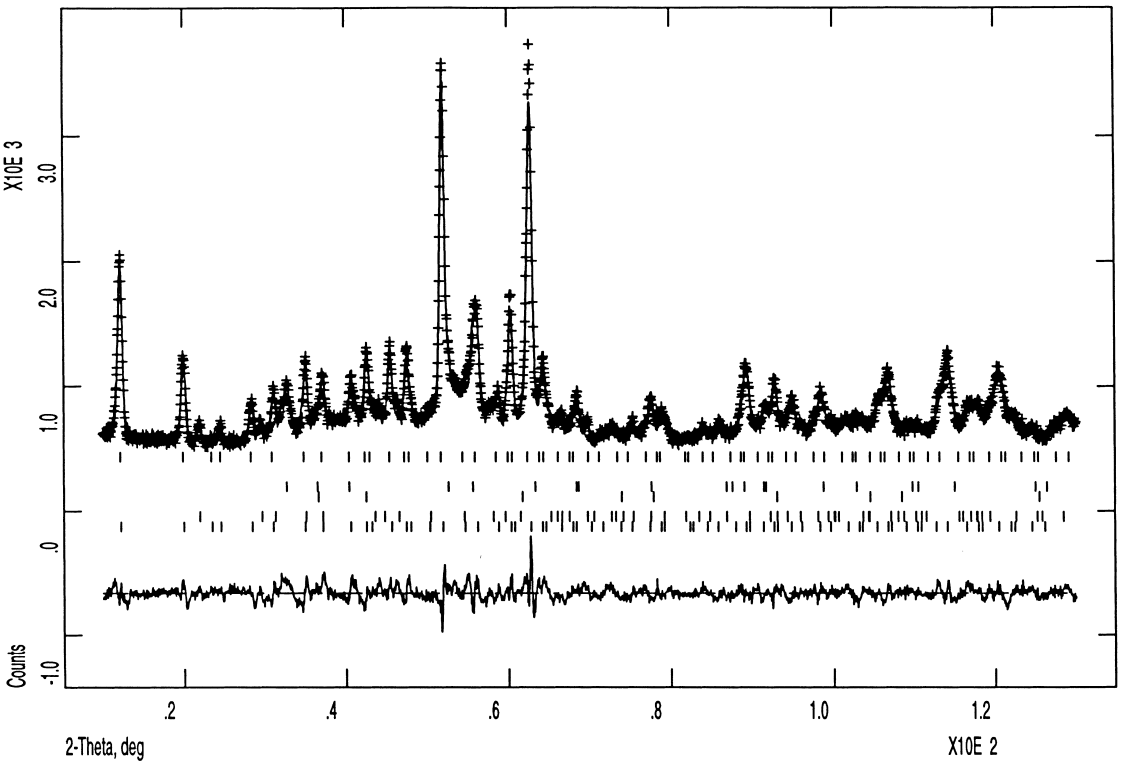

Fig. 4. Observed (+), calculated (upper line) and difference (lower line) powder neutron diffraction profile for $Zr_3V_3B_{0.40}O_{0.60}D_{6.57}$. The positions of peaks of the constituent phases are marked (from bottom to top): deuteride II, V_3B_2, VD_2, ϵ-ZrD_2 and deuteride I.

Crystal chemical analysis shows that model A can reach significantly higher theoretical value of H-storage capacity than model B [18].

In most cases, a superposition of models A and B takes place with a simultaneous partial occupation of both types of octahedra, 8*b* and 16*d*, and with all four types of tetrahedra, *D*1, *D*2, *D*3 and *D*4, partly filled. A short range order in the distribution of D atoms among the neighbouring *D*1–*D*4 tetrahedra should be assumed for such structures. The 'combined' A+B model covers deuterides II in $Zr_3V_3B_{0.40}O_{0.60}D_{6.36}$ and in $Zr_3V_3B_{0.24}O_{0.36}D_{7.96}$.

For all structure models the distances from the centres of the 8*b* and 16*d* octahedra to the neighbouring Zr_3V2 tetrahedra (*D*1 and *D*3) are in the range 1.86–2.02 Å. These values exceed significantly the corresponding shortest separations between non-bonded O and H atoms in hydrides of mixed oxides (1.68 Å in $Ti_4Fe_2OD_{2.22}$ [16]) and the O...H 'hydrogen' bond length (1.76 Å [19]). In addition, the observed distances are close to the B...H separations between nonbonded B and H in borohydrides, 1.88 Å [20]. Thus, there are no formal stereochemical limitations on simultaneous O/B occupation of octahedra and H in the *D*1–*D*4 tetrahedra in $Zr_3V_3B_{0.24}O_{0.36}D_{8.0}$ and $Zr_3V_3B_{0.40}O_{0.60}D_{6.4}$. Two possible reasons for the experimentally observed blocking in $Zr_3V_3B_{0.40}O_{0.60}D_{6.36}$ and $Zr_3V_3B_{0.24}O_{0.36}D_{7.96}$ are: (a) unfavourable changes in the local electronic density introduced by B/O in the tetrahedral sites adjusted to the occupied Zr_6 octahedra; (b) compared to reference data [16,19,20], a higher limit of the 'blocking radius' for the 'allowed' O/B...H separations (>2 Å).

The hydrogen sorption capacities of the alloys studied here are clearly related to the overall content of non transition elements in the 8*b* and 16*d* octahedra. Decreasing O+B/f.u., ongoing from $Zr_3V_3B_{0.40}O_{0.60}$ to $Zr_3V_3B_{0.24}O_{0.36}$, increases the hydrogen sorption capacity. In addition to crystal structure data and overall B+O/f.u. contents, several other parameters should be considered for optimisation of the H-storage properties of alloys in the Zr–V–B_2O_3 system. The most important are probably the conditions of H-treatment (temperature, pressure and time) during H-absorption and desorption.

4. Conclusions

Unusual transformations take place in the $Zr_3V_3B_{0.24-0.40}O_{0.36-0.60}$ alloys during hydrogen absorption–desorption cycling. The 'hydride' hydrogen increases significantly the mobility of the light nonmetalic atoms, O and B, in the face centred cubic (space group *Fd*3*m*) structures to allow hopping from 16*d* (1/2, 1/2, 1/2) into the 8*b* (7/8, 3/8, 7/8) octahedra, and a return to a nearly single occupation of the 16*d* sites for the deuterium-free alloys.

Table 1
Unit cell data, reliability factors, atomic coordinates, occupancies and temperature factors (in 10^{-2} Å^{-2}) for the deuterides of η_1-oxyboride $Zr_3B_3B_{0.24-0.40}O_{0.36-0.60}$ from Rietveld refinements of PND data at room temperature

		$Zr_3V_3B_{0.24}O_{0.36}D_{7.96}$		$Zr_3V_3B_{0.40}O_{0.60}D_{6.36}$	
		Deuteride II[a], main constituent D/f.u. = 8.05	Deuteride I[a], minor constituent D/f.u. = 7.89	Deuteride II[a], main constituent D/f.u. = 5.94	Deuteride I[a], minor constituent D/f.u. = 8.88
R_{pr}, R_{wpr}, χ^2		0.0396, 0.0515, 1.91		0.0463, 0.0576, 2.70	
a (Å)		12.7214(7)	12.7250(5)	12.6230(7)	12.698(−)
Zr in	*x*	0.5679(5)	0.5648(3)	0.5664(4)	0.5634(8)
48*f*	*n*	1(−)	1(−)	1(−)	1(−)
	U_{iso}	1.0(−)	0.8(1)	1.3(1)	0.3(−)
V1 in	*n*	1(−)	1(−)	1(−)	1(−)
16*c*	U_{iso}	1.0(−)	1.0(−)	0.5(−)	2.5(−)
V2 in	*x*	0.205(−)	0.211(4)	0.209(3)	0.210(−)
32*e*	*n*	1(−)	1(−)	1(−)	1(−)
	U_{iso}	1.0(−)	1.0(−)	0.5(−)	2.5(−)
B/O in	*n*	0.83(3)	1.00(3)	0.26(2)	1.00(−)
8*b*	U_{iso}	1.0(−)	3.2(3)	0.9(2)	0.5(−)
O/B in	*n*	0.43(3)	0.12(2)	0.80(2)	–
16*d*	U_{iso}	2.0(−)	3.7(4)	1.1(2)	
*D*1 in	*x*	0.285(2)	–	0.2901(4)	0.283(7)
32*e*	*n*	0.25(−)		0.50(2)	0.15(−)
	U_{iso}	2.0(−)		0.5(1)	2.5(−)
*D*2 in	*x*	0.130(1)	0.125(2)	0.1271(8)	0.130(3)
192*i*	*y*	0.235(2)	0.249(3)	0.2331(6)	0.237(4)
	z	0.323(2)	0.312(3)	0.3183(8)	0.316(4)
	n	0.149(9)	0.069(4)	0.184(5)	0.15(−)
	U_{iso}	2.0(−)	2.2(2)	0.04(1)	2.5(−)
*D*3 in	*x*	0.2795(4)	0.2775(2)	0.2853(6)	0.2820(8)
96*g*	*z*	0.6521(4)	0.6502(3)	0.6521(8)	0.6551(7)
	n	0.75(−)	0.777(10)	0.348(9)	0.78(4)
	U_{iso}	2.0(−)	1.6(1)	3.4(3)	0.8(−)
*D*4 in	*x*	0.344(1)	0.3497(4)	0.341(2)	0.358(1)
96*g*	*z*	0.027(2)	0.0321(8)	0.017(2)	0.036(2)
	n	0.21(1)	0.40(1)	0.108(5)	0.35(−)
	U_{iso}	2.0(−))	1.5(1)	1.9(2)	0.5(−)
Zr–D (Å)		1.98(2)–2.08(1)	1.95(3)–2.06(1)	1.93(1)–2.19(3)	1.94(3)–2.09(5)
V–D (Å)		1.72(2)–1.90(2)	1.75(4)–1.83(7)	1.63(3)–1.83(1)	1.61(3)–1.98(2)
Zr–O (Å)		2.409(2)	2.396(1)	2.384(2)	–
Zr–B (Å)		2.454(6)	2.415(4)	2.416(5)	2.392(11)
O–D (Å)		2.006(6)	1.974(4)	2.02(1)	–
B–D (Å)		1.99(4)	2.763(4)	1.857(9)	2.02(13)

[a] Approximate relative amounts deuteride I/deuteride II = 7/8 ($Zr_3V_3B_{0.24}O_{0.36}D_{7.96}$) and 1/6 ($Zr_3V_3B_{0.40}O_{0.60}D_{6.36}$). Space group $Fd\bar{3}m$ (No. 227). Calculated standard deviations in parentheses. Atoms occupy the following positions: 48*f* (*x*,3/8,3/8), 16*c* (0,0,0), 32*e* (*x*,*x*,*x*), 8*b* (7/8,3/8,7/8), 16*d* (1/2, 1/2, 1/2), 192*i* (*x*,*y*,*z*), 96*g* (*x*,*x*,*z*).

The redistribution of O/B within the 16*d* and 8*b* sites gives significantly different deuterium sublattices in $Zr_3V_3B_{0.24}O_{0.36}D_{8.0}$ and $Zr_3V_3B_{0.40}O_{0.60}D_{6.4}$ deuterides compared to the chemically similar $Zr_3V_3OD_{4.93}$ [15], with O only in the 16*d* octahedra.

The observed blocking of D insertion into the Zr_3V tetrahedra connected to the O/B-filled Zr_6 octahedra leads to the conclusion that hydrogen storage capacity reaches the highest values for the $Zr_3V_3(B,O)_{\leq 0.5}$ oxyborides with only 8*b* site occupied by O/B.

Acknowledgements

We thank Professor G. Wiesinger (TU Vienna) for the kind provision of the isotope-pure boron oxide, $^{11}B_2O_3$. We

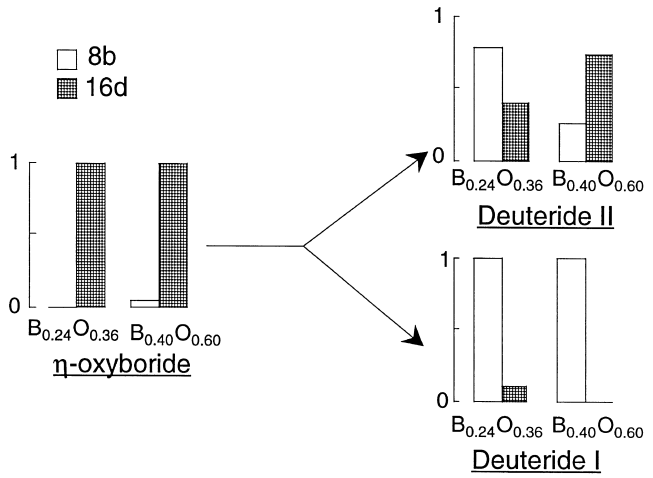

Fig. 5. Change of the relative occupancies of the 8*b* and 16*d* octahedra by B and O atoms on deuteration of the η_1-oxyboride.

appreciate the cooperation and fruitful discussions with Professor I.R. Harris, Dr P.W. Guegan (The University of Birmingham) and Professor H. Fjellvåg (Oslo University).

References

[1] V.A. Yartys, I.Yu. Zavaliy, M.V. Lototzky, Koord. Khimiya (Sov. J. Coord. Chem.) 18 (4) (1992) 409.
[2] V.A. Yartys, I.Yu. Zavaliy, M.V. Lototzky, A.B. Riabov, Yu.F. Shmalko, Z. Phys. Chem. 183 (1994) 465.
[3] A.B. Riabov, V.A. Yartys, B.C. Hauback, P.W. Guegan, G. Wiesinger, I.R. Harris, J. Alloys Comp. 293–295 (1999) 93.
[4] A.C. Larson, R.B. von Dreele, General Structure Analysis System, LANL, 1994.
[5] V.F. Sears, Neutron News 3 (1992) 26.
[6] S.S. Sidha, N.S. Satya Murthy, F.P. Campos, D.D. Zauberis, Adv. Chem. Ser. 39 (1963) 87.
[7] H. Müller, K. Weymann, J. Less-Common Metals 119 (1986) 115.
[8] J.-J. Didisheim, K. Yvon, P. Fischer, D. Shaltiel, Solid State Commun. 38 (1981) 637.
[9] E. Rudy, F. Benessovsky, L. Toth, Z. Metallk. 54 (1963) 345.
[10] R.E. Spear, P.W. Gilles, High Temp. Sci. 1 (1969) 86.
[11] L.M. Kovba, I.I. Kornilov, E.M. Kenina, V.V. Glazova, Doklady AN SSSR 180 (1968) 360, in Russian.
[12] M. Marezio, J.P. Remeika, P.D. Dernier, Acta Crystallogr. B 26 (1979) 2008.
[13] S.V. Berger, Acta Chem. Scand. 7 (1953) 611.
[14] Yu.B. Kuz'ma, Crystal Chemistry of Borides, Vyszcza Szkola, Lviv, 1983, 160 p.
[15] F.J. Rotella, H.E. Flotow, D.M. Gruen, J.D. Jorgensen, J. Chem. Phys. 79 (1983) 4522.
[16] C. Stioui, D. Fruchart, A. Rouault, R. Fruchart, E. Roudaut, J. Rebiére, Mater. Res. Bull. 16 (1981) 869.
[17] J.L. Soubeyroux, D. Fruchart, S. Derdour, P. Vuillet, A. Rouault, J. Less-Common Metals 129 (1987) 187.
[18] A.B. Riabov, V.A. Yartys, to be published.
[19] A.B. Riabov, PhD thesis, Lviv (1997) 152 p.
[20] R.D. Dobrott, L.B. Friedman, W.N. Lipscomb, J. Chem. Phys. 40 (1964) 866.